# Well-Defined Amphiphilic Double-Brush Copolymers and Their Performance as Emulsion Surfactants

**ARTICLE** *in* MACROMOLECULES · JUNE 2012

Impact Factor: 5.8 · DOI: 10.1021/ma300565j



**5 AUTHORS**, INCLUDING:

Jiong Zou
Texas A&M University
**33** PUBLICATIONS **631** CITATIONS
SEE PROFILE

Biswa P. Das
University at Buffalo, The State University of N…
**15** PUBLICATIONS **84** CITATIONS
SEE PROFILE

Macromolecules

Article

pubs.acs.org/Macromolecules

# Well-Defined Amphiphilic Double-Brush Copolymers and Their Performance as Emulsion Surfactants

Yukun Li, Jiong Zou, Biswa P. Das, Marina Tsianou, and Chong Cheng*

Department of Chemical and Biological Engineering, The State University of New York, Buffalo, New York 14260, United States

Supporting Information

**ABSTRACT:** Amphiphilic double-brush copolymers (DBCs) with each graft site quantitatively carrying both a hydrophilic poly(ethylene oxide) (PEO) graft and a hydrophobic polylactide (PLA) graft were synthesized, characterized, and further utilized as surfactants for the stabilization of miniemulsions. Well-defined PEO-*b*-PLA-based diblock macromonomers (MMs) with *exo*-norbornene (NB)-functionalized diblock junction were prepared by the synthesis of a PEO-based NB-functionalized alcohol via polymeric reaction, followed by ring-opening polymerization (ROP) of lactide (LA) initiated by the alcohol. Ring-opening metathesis polymerization (ROMP) of the MMs yielded DBCs. The well-controlled structures of the MMs and the DBCs were verified through rigorous instrumental characterizations. As compared with the MMs, the corresponding DBCs had lower crystallinities and melting temperatures ($T_m$s) for both PEO and PLA phases and showed a negligible tendency for intermolecular self-assembly in solutions. With nanoscopic dimensions and novel amphiphilic architectures, these DBCs represent a new type of giant polymeric surfactant. Relative to the precursor MMs, the DBCs resulted in miniemulsions with remarkably enhanced stability.

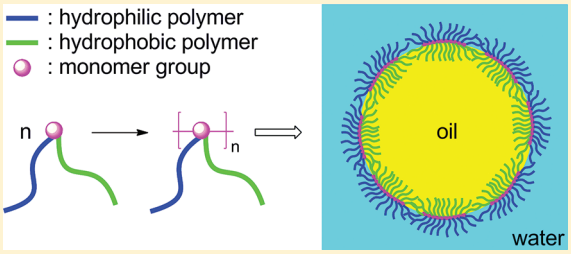


## INTRODUCTION

Amphiphiles with both hydrophilic and hydrophobic components have been broadly used as surfactants. Relative to small molecule amphiphiles, polymeric amphiphiles can result in interfacial assemblies with enhanced dynamic stability.[1] Moreover, Janus polymeric amphiphiles may lead to nanostructured interfacial layers with interesting properties.[2] Several types of Janus polymeric amphiphiles have been synthesized and studied as surfactants. Amphiphilic Janus dendrimers were first obtained by Fréchet and co-workers through convergent approach, and such dendrimers may effectively stabilize the water−oil interface of emulsion.[3] Schlüter and co-workers prepared amphiphilic Janus dendronized polymers by the polymerization of a monomer-functionalized Janus dendrimer and found both the precursor dendrimer and the resulting dendronized polymers can form stable Langmuir monolayers at the air/water interface.[4] Müller and co-workers synthesized amphiphilic Janus nanoparticles by selective cross-linking of Janus micelles of triblock copolymers and further utilized these Janus nanoparticles as stabilizer for emulsion polymerization or polymer blends.[5,6]

Heterografted brush copolymers with both hydrophilic and hydrophobic grafts have attracted significant attention because of their interesting structures and special properties.[7−10] Brush block copolymers can possess blockwise unimolecular Janus conformations[11] as well as intermolecularly assembled nanostructures.[12−14] Brush statistical copolymers have been speculated to possess Janus conformations through intramolecular self-assembly,[14−25] but verification of their Janus nanostructures by direct visualization of distinguishable nonenclosed nanoscopic domains of individual macromolecules is very challenging.[26] Although amphiphilic heterografted brush copolymers can form assembled nanostructures in solutions,[12,21−23] their application as surfactants to stabilize biphasic systems has not been reported. Moreover, because the individual covalent bonds on backbone of brush polymers can break due to the presence of significant tension along backbone,[27] the backbone block junctions of brush block copolymers may be vulnerable at interfaces due to the concentrated interfacial tension.

We have synthesized DBCs, a novel type of heterografted brush copolymer with each graft site quantitatively carrying two different grafts, by "grafting through" diblock MMs with monomer-functionalized block junctions and verified DBCs as a new class of Janus nanomaterials through the visualization of their Janus nanostructures.[26,28] In our previous studies, such diblock MMs were prepared through anionic polymerization or simultaneous living polymerizations. However, because anionic polymerization requires stringent reaction conditions and simultaneous living polymerizations need high compatibility of two different polymerization systems, the compositions of the resulting diblock MMs were considerably restricted. Thus, to obtain a broad variety of DBCs, we intend to develop new approaches for the preparation of such diblock MMs. We are particularly interested in DBCs with both hydrophilic and hydrophobic grafts because of their promising application as

**Received:** March 19, 2012
**Revised:** May 8, 2012
**Published:** May 18, 2012

surfactants. As amphiphilic Janus nanomaterials, they may help to stabilize biphasic systems by selective interactions of these heterografts with different phases. With numerous amphiphilic junctions per molecule, they have also robust structures to withstand high interfacial tension.

Recently, we have also investigated miniemulsion systems using different types of surfactants for template synthesis.[29−31] Without enhancing template stability through crystallization, interfacial cross-linking of small molecule surfactant monolayers of oil-in-water miniemulsions gave only ill-defined products;[29] on the other hand, interfacial cross-linking of the monolayers of amphiphilic diblock polymeric surfactants readily yielded well-defined nanocapsules.[30] The results suggested that emulsion stability may positively correlate with the size of surfactant molecules. Because DBCs can be considered as the giant macromolecules with diblock copolymer as repeat unit, a hypothesis that, relative to amphiphilic diblock copolymers, DBCs with both hydrophilic and hydrophobic grafts may result in emulsions with higher stability can be proposed.

In this article, we report the synthesis and characterization of the first examples of amphiphilic DBCs obtained from the corresponding amphiphilic diblock MMs and the study of their performance as miniemulsion surfactants. Different from our previous work, the approach of tandem polymeric reaction and living polymerization was employed to prepare the amphiphilic PEO/PLA-based diblock MMs. The emulsions using the diblock MMs and their resulting amphiphilic DBCs as surfactants were investigated in order to examine the hypothesis. To the best of our knowledge, this is the first report to compare amphiphilic heterografted brush copolymers and their precursor amphiphilic block copolymers in the performance to stabilize biphasic systems.

## RESULTS AND DISCUSSION

The synthetic route for the preparation of PNB-*g*-PEO/PLA amphiphilic DBCs is shown in Scheme 1. The "grafting through" approach was selected to guarantee the quantitative grafting of both hydrophilic PEO and hydrophobic PLA grafts, and accordingly well-defined PEO-*b*-PLA diblock MMs with monomer group at block junctions need to be synthesized by tandem polymeric reaction and ROP at first.[32] The *exo*-NB group was chosen as the monomer functionality for the MMs because of its high reactivity in ROMP.[26,33−35] A tetraethylene glycol-based spacer was utilized to link the NB group and the diblock junction of MMs in order to maintain the high reactivity of the MMs by reducing steric hindrance toward NB.

To prepare the MMs, $\omega$-acid-functionalized $PEO_{45}$ (**1**) and an *exo*-NB-based diol (**2**) were synthesized at first.[36] The esterification of **1** with an excess of **2** (4.0 equiv) was catalyzed by dicyclohexylcarbodiimide (DCC) and 4-(dimethylamino)-pyridinium 4-toluenesulfonate (DPTS) at room temperature (rt) for over 12 h and gave a well-defined PEO-based NB-functionalized alcohol (**3**; $PEO_{45}$-NB-OH, $M_n^{NMR}$ = 2.55 kDa, $PDI^{GPC}$ = 1.02), the monoesterified product, in 86% yield.[37] The chemical structure of **3** was confirmed by $^1H$ NMR analysis (Figure 1a). Matrix-assisted laser desorption ionization time-of-flight (MALDI-TOF) analysis showed that **3** had a $M_n$ of 2.39 kDa and a narrow PDI of 1.06 (Figure 2). Catalyzed by 4-(dimethylamino)pyridine (DMAP),[38] living ROP of L-lactide (LA) using the hydroxyl group of **3** as initiator functionality was conducted in $CH_2Cl_2$ at 35 °C for 15−24 h ($[LA]_0$:$[3]_0$:$[DMAP]_0$ = 13−50:1:4; Table 1). With high monomer conversions (78−85%), PEO-NB-PLA diblock MMs (**4**) with

**Scheme 1. Synthesis of Amphiphilic DBCs, PNB-*g*-PEO/PLA**

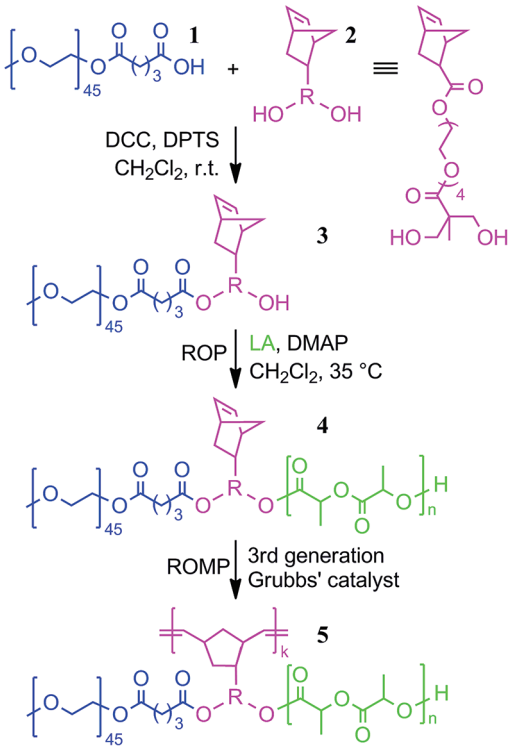


well-controlled structures ($M_n^{NMR}$ = 4.26−8.90 kDa, $PDI^{GPC}$ = 1.03−1.10) were obtained. The $DP_n$ values for their PLA blocks were determined by $^1H$ NMR analysis based on the comparison of the resonance intensities of the CH protons from PLA at 5.12−5.40 ppm with these of CH═CH protons from NB group at 6.08−6.17 ppm (Figure 1b). The experimental $DP_n$ values of 12−44 were in close agreement with the theoretical $DP_n$ values of 11−42 calculated from $[LA]_0$:$[3]_0$ and conversions of LA, further indicating the well-controlled formation of the PLA blocks. The well-defined diblock structures of the MMs were also supported by their narrow and monomodal GPC curves (Figure 3). MALDI-TOF analysis showed that **4a** had a $M_n$ of 4.28 kDa with a PDI of 1.03, and **4b** had a $M_n$ of 5.57 kDa with a PDI of 1.05. In close agreement with the $M_n^{NMR}$ and $PDI^{GPC}$ data, these $M_n^{MALDI}$ and $PDI^{MALDI}$ values confirmed the precisely controlled synthesis of **4a** and **4b**. Under the same measurement conditions, precise MALDI-TOF analysis could not be achieved for **4c**, presumably because the higher $M_n$ of **4c** made the vaporization of **4c** macromolecules more difficult.

Sequentially, amphiphilic DBCs (**5**), i.e. PNB-*g*-PEO/PLA, were synthesized by ROMP of MMs **4** using the third generation Grubbs' catalyst as initiator in $CH_2Cl_2$ at rt for 1 h ($[4]_0$:$[Ru]_0$ = 50−250; Table 2). As determined by GPC analysis of polymerization solutions based on the peak areas of DBCs and the remaining MMs, high conversions of **4** were obtained in most trials. The conversions of **4** noticeably decreased with the increase of molecular size of **4**, as well as $[4]_0$:$[Ru]_0$. Pure DBCs were obtained after passing polymerization solutions through short columns of silica gel to trap unreacted MMs (Figure S1).[39] Well-defined structures of DBCs were verified by their narrow and monomodal GPC curves (Figure 3; PDI = 1.11−1.23). Moreover, the good agreement of the PLA and PEO protons before and after ROMP process and


dx.doi.org/10.1021/ma300565j | *Macromolecules* 2012, 45, 4623−4629

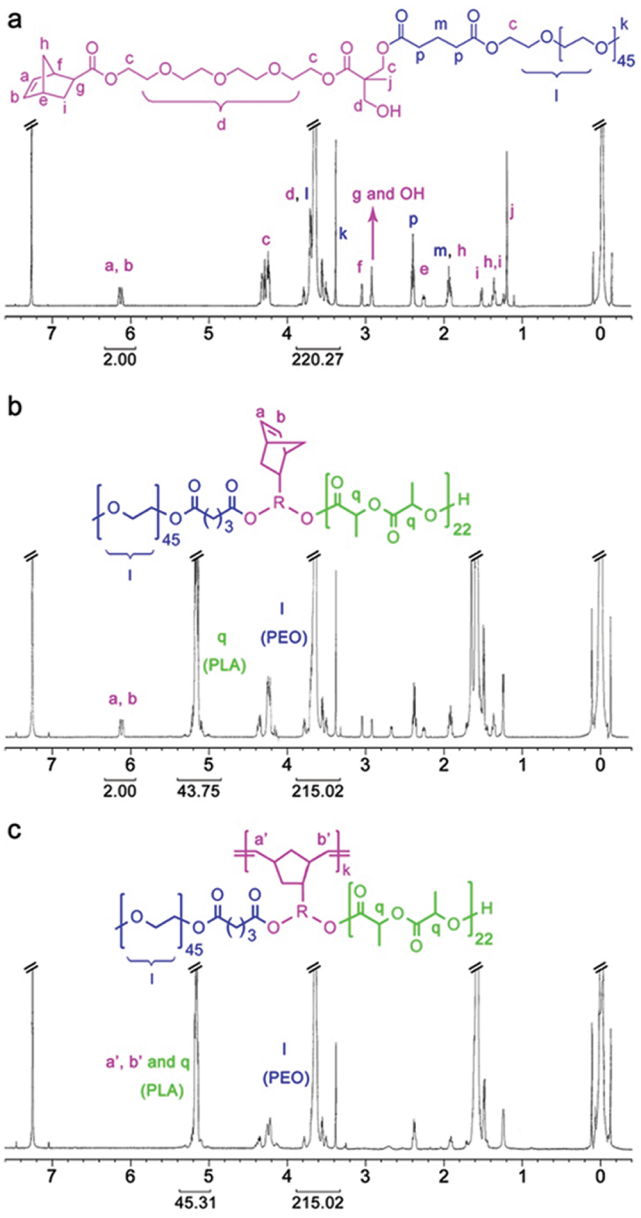


**Figure 1.** $^1$H NMR spectra of (a) macroinitiator **3**, (b) diblock MM **4b**, and (c) DBC **5b2**.

the disappearance of the CH═CH protons from NB group in DBCs were verified by $^1$H NMR analysis (Figure 1c) provided further evidence for well-controlled ROMP process. The $M_n^{GPC}$ values of DBCs were somewhat higher than the $M_n$ values calculated from $[4]:[Ru]_0$ and conversions of **4**. Because the

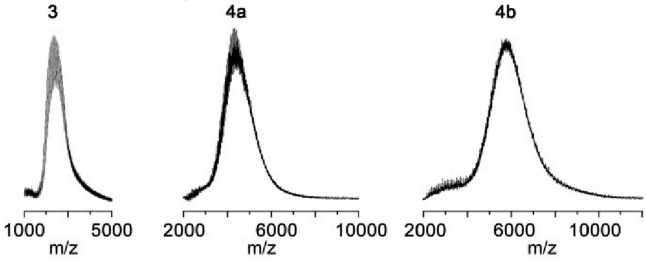


**Figure 2.** MALDI-TOF spectra of macroinitiator **3** and diblock MMs **4a** and **4b**.

**Table 1. Synthesis of PEO-NB-PLA Diblock MMs**[a]

| entry | $[LA]_0/[3]_0$ | conv, %[b] (LA) | $DP_{n,PLA}$ $^1$H NMR | $DP_{n,PLA}$ calcd | $M_n$[b], kDa | PDI[c] |
|---|---|---|---|---|---|---|
| **4a** | 13 | 85 | 12 | 11 | 4.26 | 1.03 |
| **4b** | 25 | 78 | 22 | 20 | 5.70 | 1.05 |
| **4c** | 50 | 83 | 44 | 42 | 8.87 | 1.10 |

[a]Polymerization conditions: $[3]_0:[DMAP]_0$ = 1:4, in $CH_2Cl_2$, 35 °C, 15−24 h. [b]By $^1$H NMR analysis. [c]By GPC using RI detector, relative to linear polystyrenes.

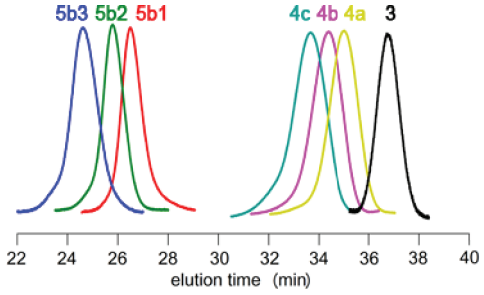


**Figure 3.** GPC curves of macroinitiator **3**, diblock MMs **4a−c**, and amphiphilic DBCs **5b1−3** (prepared from **4b**).

**Table 2. Synthesis of PNB-*g*-PEO/PLA Amphiphilic DBCs**[a]

| entry | MM | $[4]_0/[Ru]_0$ | conv, %[b] (MM) | $M_n$, kDa calcd | $M_n$, kDa GPC[c] | PDI[c] | $D_h$[d], nm |
|---|---|---|---|---|---|---|---|
| **5a1** | **4a** | 50 | 100 | 213 | 276 | 1.11 | 16.2 |
| **5a2** | **4a** | 100 | 83 | 354 | 488 | 1.15 | 23.1 |
| **5a3** | **4a** | 250 | 82 | 873 | 1090 | 1.23 | 30.0 |
| **5b1** | **4b** | 50 | 96 | 274 | 342 | 1.12 | 21.9 |
| **5b2** | **4b** | 100 | 81 | 462 | 633 | 1.13 | 23.3 |
| **5b3** | **4b** | 250 | 72 | 1030 | 1700 | 1.16 | 31.5 |
| **5c1** | **4c** | 50 | 84 | 373 | 525 | 1.12 | 23.2 |
| **5c2** | **4c** | 100 | 77 | 683 | 967 | 1.11 | 26.2 |
| **5c3** | **4c** | 250 | 49 | 1090 | 1730 | 1.13 | 32.5 |

[a]Polymerization conditions: rt, 1 h, in $CH_2Cl_2$. [b]By GPC using RI detector. [c]By GPC using multiple detectors. [d]In toluene, by DLS.

living characteristic of the ROMP process was verified by a sequential MM addition experiment (see Figure S2), the differences between the experimental and calculated $M_n$ values were ascribed to the minor losses of initiator at the initiation stage. Using **5b1−3** as representative samples, tapping mode AFM characterization of DBCs on mica verified their well-defined nanostructures (Figure 4). Sample **5b1** exhibited flattened short cylindrical morphologies with an average length 36 ± 5 nm, an average width of ∼18 nm, and surface height of ∼0.3 nm. With the increase of the length ratios of backbone to

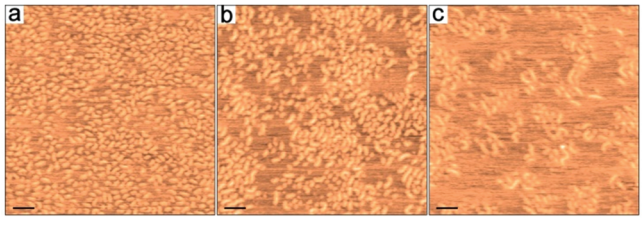


**Figure 4.** Tapping mode AFM height images of (a) **5b1**, (b) **5b2**, and (c) **5b3** (scale bar: 50 nm; height scale: 0.8 nm).


dx.doi.org/10.1021/ma300565j | *Macromolecules* 2012, 45, 4623−4629

grafts relative to **5b1**, samples **5b2** and **5b3** showed similar surface heights but increased length−height aspect ratios. However, relative to the DBCs with both polystyrene (PSt) and PLA grafts (i.e., PNB-*g*-PSt/PLA) which we reported previously,[26] the current PNB-*g*-PEO/PLA samples with comparable PNB backbone length exhibited significantly shorter surface length by AFM imaging. The result might be ascribed to that, as compared with the PSt grafts of PNB-*g*-PSt/PLAs, the PEO grafts of PNB-*g*-PEO/PLAs were not only more flexible and would not cause substantial steric effects to stiffen backbones, but also more hydrophilic and could be strongly adsorbed by mica surface to promote the spontaneous adsorption-induced scission of carbon−carbon bonds of DBC backbones.[27] The presence of Janus conformations showing two distinguishable nanoscopic domains within individual DBC macromolecules on the *x*−*y* plane was not observed, presumably because of the selective adsorption of their PEO grafts by the highly polar mica surface.[26]

Using precursor MMs **4** as controls, the bulk and solution properties of amphiphilic DBCs **5** were characterized. According to DSC analysis, as compared with MMs, the corresponding DBCs had lower crystallinities and $T_m$s for both PEO and PLA domains (Figure 5). For instance, MM **4b** had

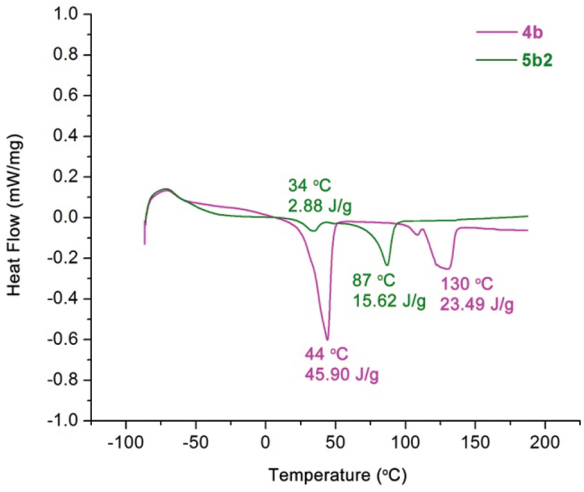


**Figure 5.** DSC measurements for MM **4b** and DBC **5b2** (heating rates: 10 °C/min).

70% crystallinity for PEO phase with a $T_m$ of 44 °C and 42% crystallinity for PLA phase with a $T_m$ of 130 °C; prepared from **4b**, DBC **5b2** possessed only about 4% crystallinity for PEO phase with a $T_m$ of 34 °C and 28% crystallinity for PLA phase with a $T_m$ of 87 °C. The crystallinity values were obtained through normalizing fusion enthalpy ($\Delta H_f$) values of samples by dividing them with the mass fractions of PEO (0.351) or PLA (0.556) in the copolymers, followed by comparing the normalized values with the $\Delta H_f$ values for 100% crystalline polymers ($\Delta H_{f,\,PEO}$ = 188 J/g; $\Delta H_{f,\,PLA}$ = 101 J/g).[40] Because crystallization of polymers requires regular packing of polymer chains realized through effective chain motions, the results suggested that the presence of polymer backbone in DBCs may significantly hinder the motions of the tethered PEO and PLA grafts and restrict them from regular packing.

Different solubility and/or solution behavior between DBCs and MMs were observed in organic solvents, such as toluene, ethyl acetate, and THF (Figure 6). DBCs had hydrodynamic diameter ($D_h$) of 16.2−32.5 nm in toluene at rt. However,

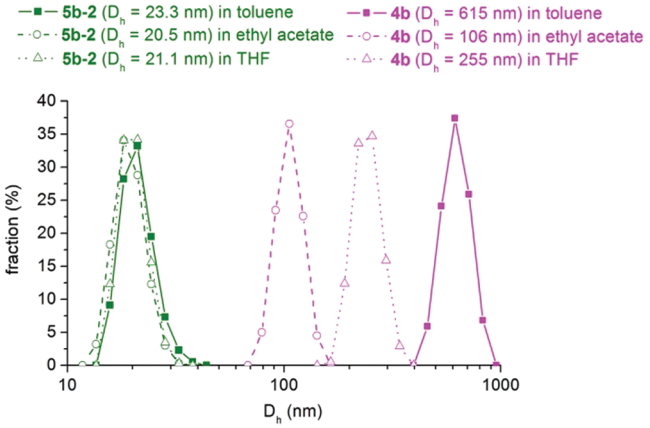


**Figure 6.** DLS results of **4b** and **5b2** in toluene, ethyl acetate, and THF.

under the same conditions, MM **4a** and **4b** formed intermolecular assemblies in toluene according to their $D_h$ values obtained by DLS analysis, and **4c** can only be swollen by toluene. Similarly, DBCs had $D_h$ values around 15−30 nm in ethyl acetate and THF, while their precursor MMs exhibited much larger assembled structures with $D_h$ over 100 nm in these solvents. The results suggested that DBCs had smaller secondary interchain force and lower tendency for intermolecular self-assembly than MMs in organic solvents.

With amphiphilic structures, DBCs and MMs exhibited different assembly behavior in water. Self-assemblies of MMs were obtained by slow additions of water into dilute DMF solutions of the polymers followed by dialysis against water (Figure 7), and their $D_h$ values (164 nm for **4a**, 79 nm for **4b**,

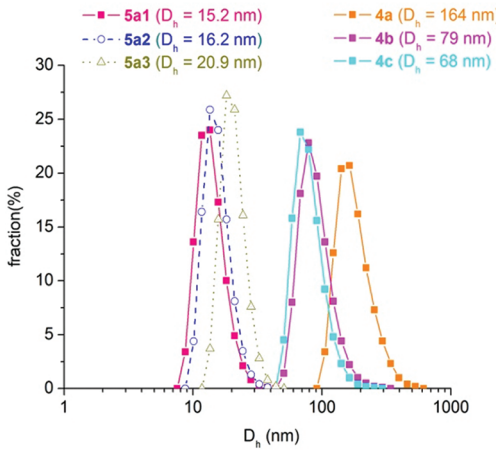


**Figure 7.** DLS results of MMs **4a**, **4b**, **4c** and DBCs **5a1**, **5a2**, **5a3** in water.

68 nm for **4c**) determined by DLS indicated the formation of intermolecular aggregates of these MMs in water.[12] Following the same protocol, only DBCs **5a1**−**3** (PNB-*g*-$PEO_{45}$/$PLA_{12}$; 46.9 wt % of PEO) were dispersible in water. As compared with their $D_h$ values in toluene (16.2 nm for **5a1**, 23.1 nm for **5a2**, and 30.0 nm for **5a3**), their smaller $D_h$ values in water (15.2 nm for **5a1**, 16.2 nm for **5a2**, and 20.9 nm for **5a3**) suggested that, with much longer PEO grafts than PLA grafts, the DBCs **5a1**−**3** presented as unimolecular micelles with water-soluble PEG-based shell domains and water-insoluble PLA-enriched collapsed cores. On the other hand, DBCs **5b1**−**3** (PNB-*g*-


dx.doi.org/10.1021/ma300565j | *Macromolecules* 2012, 45, 4623−4629

$PEO_{45}/PLA_{22}$; 35.1 wt % of PEO) and DBCs **5c1−3** (PNB-*g*-$PEO_{45}/PLA_{44}$; 22.5 wt % of PEO) precipitated in water because their insufficient PEO fractions would not allow the formation of PEG-based shell for affording good water dispersibility of the macromolecules with increased PLA graft lengths. The results further indicated that, relative to MMs, DBCs also had lower tendency to form dispersible intermolecular self-assemblies in water.

Because DBCs are not prone to intermolecularly self-assemble in various solvents, potentially DBCs may have facilitated interactions with solvents for enhanced performance as surfactants. Using **5b1−3** and **4b** as representatives of DBC samples and MM references, the performance of DBCs as emulsion surfactants to stabilize water−oil (W/O) interfaces was investigated. Because miniemulsions have important applications in polymer field,[29−31,41−43] miniemulsion systems were selected in this study. After miniemulsions were prepared using toluene as the major component of oil and hexadecane (HD) as the hydrophobe ($W_{toluene}$:$W_{HD}$:$W_{DBC/MM}$ = 20:2:1; $V_W$:$V_{toluene/HD}$ = 225:1; 20 min of ultrasonication; rt),[41] the diameters of oil droplets in miniemulsions were monitored by DLS (Figure 8). For each trail, average cross-sectional

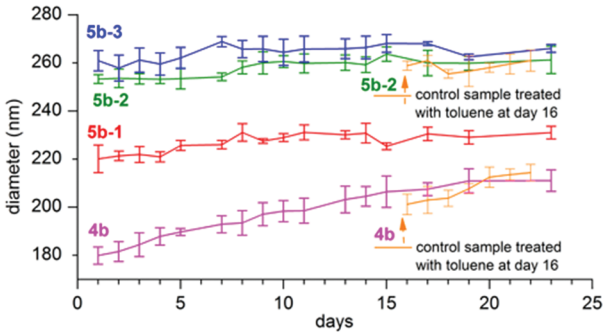


**Figure 8.** Time-dependent variations of droplet diameters in the miniemulsions prepared using DBCs **5b1−3** and MM **4b** as surfactants.

interfacial area stabilized by surfactant ($A_{surf}$) was calculated.[5] With densely grafted amphiphilic architectures, the MM units of **5b1−3** had $A_{surf}$ values of 6.8 ± 0.2, 5.9 ± 0.1, and 5.7 ± 0.1 $nm^2$ at day 1, a little lower than the $A_{surf}$ of **4b** of 8.3 ± 0.2 $nm^2$. Considering the backbone $DP_n$ of these DBCs (which can be estimated as the ratio of $M_{n,5}/M_{n,4}$), the $A_{surf}$ values of **5b1−3** molecules were about 410, 650, and 1700 $nm^2$, respectively. The much larger $A_{surf}$ values of **5b1−3** relative to **4b** suggested that the surfactant layers of DBCs potentially may lead to significant resistance of the diffusion of nanoscopic substances through the W/O interfaces.

As indicators of miniemulsion stability, the time-dependent variations of droplet diameters were tracked. As compared with **4b**, **5b1−3** resulted in much more stable miniemulsions. For the miniemulsion using **4b** as surfactant, droplet diameter increased steadily by 17% from day 1 to day 23, corresponding to the same extent of drop in surfactant efficiency. On the other hand, the miniemulsions using **5b1−3** as surfactants showed only 2−5% increases of droplet diameters during the same time period. The DBC-based miniemulsions also exhibited higher stability toward environmental changes. As control experiments, toluene top layers were introduced to two miniemulsion systems at day 16. In the next 6 days, droplet diameter increased by 7% for the **4b**-based system, but the maximum variation of droplet diameter was only 2% for the **5b2**-based system. These surfactants were chemically stable under the miniemulsion conditions (Figure S3). Three factors may contribute to the high stability of the DBC-based miniemulsions. First, because **5b1−3** were not water-dispersible and had high MWs, their diffusion in water, the continuous phase of miniemulsions, was highly restricted. Second, coalescence of droplets can be suppressed by the low secondary forces between DBC molecules. Third, because DBCs can serve as more effective diffusion barriers than MMs, the suppression of Ostwald ripening was enhanced.[41] It should be noted that, because hydrophobicity of PLA chains is not particularly high, the presence of hydrophobe is still critical for promoting interfacial tension and further suppressing Ostwald ripening in the miniemulsions. For both DBC and MM-based miniemulsions without hydrophobe, miniemulsion nanodroplets showed broad size distributions.

## ■ CONCLUSIONS

We have demonstrated that well-defined DBCs can be prepared by the synthesis of well-defined NB-functionalized diblock MMs by tandem polymeric reaction and ROP, followed by ROMP "grafting through" of the MMs. Relative to the amphiphilic precursor MMs, amphiphilic DBCs with each graft junction carrying a hydrophilic graft and a hydrophobic graft exhibited lower crystallinities and $T_m$ values as well as less tendency for intermolecular self-assembly. Having nanoscopic molecular sizes and novel amphiphilic structures, the DBCs represent a new class of giant macromolecular surfactant and can lead to the formation of miniemulsions with unusually high stability. Potentially, they may be used to stabilize the interfaces of a variety of biphasic systems, including other types of emulsions and polymer blends;[5] they may also have other interesting applications, such as the preparation of "breathable" Langmuir films.[2,44]

## ■ EXPERIMENTAL SECTION

**Measurements.** $^1$H NMR (500 MHz) spectra were acquired in $CDCl_3$ using a Varian INOVA-500 spectrometer at 25 °C. Tetramethylsilane (TMS) was used as an internal reference for $^1$H NMR spectroscopy.

Matrix-assisted laser desorption/ionization time-of-flight (MALDI-TOF) mass spectrometry was measured on a Bruker Biflex IV (Billerica, MA) MALDI mass spectrometer equipped with a nitrogen laser ($\lambda$ = 337 nm). The mass spectrum was acquired in the reflection mode with a mass range of 1000−12 000 $m/z$, and the mass scale was calibrated externally using the peaks of peptide calibration standard II purchased from Bruker. *trans*-2-[3-(4-*tert*-Butylphenyl)-2-methyl-2-propenylidene]malononitrile (DCTB, ≥99%; Aldrich) served as the matrix and was dissolved in $CHCl_3$ at a concentration of 20 mg/mL. Sodium trifluoroacetate (NaTFA, 98%; Aldrich) served as the cationizing agent and was dissolved in MeOH/$CHCl_3$ (1/3, v/v) at a concentration of 10 mg/mL. The polymer was dissolved in $CHCl_3$ at a concentration of 10 mg/mL. The matrix solution, polymer solution, and NaTFA solution were mixed in the ratio of 10/1/1 (v/v/v). The sample preparation involved depositing 1 $\mu$L of the mixture on the steel plate and allowing the spot to dry.

Gel permeation chromatography (GPC) was conducted using Viscotek GPC system equipped with a VE-3580 refractive index (RI) detector, a 270 dual detector system having a viscometer detector and a dual-angle (7° and 90°) laser light scattering (LS) detector, a VE 1122 pump, and two mixed-bed organic columns (PAS-103 M with exclusion limit of 70 kDa and PAS-105 M with exclusion limit of 4 MDa). *N*,*N*′-Dimethylformamide (HPLC grade) with 0.1 M LiBr was used as solvent for polymers and eluent for GPC with a flow rate of


dx.doi.org/10.1021/ma300565j | *Macromolecules* 2012, 45, 4623−4629

0.50 mL/min at 55 °C. Polymer solutions were prepared at a known concentration (ca. 3 mg/mL), and an injection volume of 100 μL was used. The system was calibrated with linear polystyrene standards with narrow polydispersities (PDI < 1.1; Polymer Laboratories, Varian Inc.). For GPC analysis of MMs, their MWs and MW distributions were obtained based on the responses from the RI detector only because the LS detector from the 270 dual detector system was not sensitive enough for polymer species with MW less than ~5 kDa. For GPC analysis of double-brush copolymers (DBCs), their MWs and MW distributions were obtained based on the responses from both the RI detector and the 270 dual detector system.

Atomic force microscopy (AFM) were performed on an Asylum Research MFP-3D AFM instrument operating in tapping mode. The measurements were conducted in air at ambient conditions by using Si cantilevers with a spring constant of ca. 20−95 N/m and a resonance frequency of about 145−230 kHz, with image resolution of 512 × 512 points and a scan rate of 1 Hz. The AFM tip was purchased from Nanoscience Instruments with a radius of smaller than 10 nm. The AFM samples were prepared from dilute sample solutions (0.02−0.1 mg/mL in $CH_2Cl_2$) by spin-coating on freshly cleaved mica.

Dynamic light scattering measurements were performed using a Nano ZS90 Zetasizer (Malvern Instruments). A 4 mW 633 nm HeNe laser was used as the light source, and all experiments were performed at a temperature of 25.0 °C at a measuring angle of 90° to the incident laser beam. The correlation decay functions were analyzed by cumulants method to obtain size distribution. All determinations were repeated five times.

Thermogravimetric analysis (TGA) was performed on a TG209F1 instrument (Nettzsch, Inc.) measuring the total mass loss on ~6 mg sample from 25 to 550 °C at a heating rate of 10 °C/min in a nitrogen flow of 50 mL/min. Differential scanning calorimetry (DSC) was operated on a TA Instruments Q200 system with a RCS-90 cooling device in a temperature range of −90 to 200 °C under nitrogen. The samples were quenched from 40 to −90 °C with a cooling rate of 10 °C/min. After holding at −90 °C for 5 min, the samples were heated to 200 °C with a heating rate of 10 °C/min, followed by quenched to −90 °C with a cooling rate of 10 °C/min. The operation was conducted for two cycles.

**Materials.** 4-(Dimethylamino)pyridine (DMAP; 99+%), *N,N′*-dicyclohexylcarbodiimide (DCC, 99%), *p*-toluenesulfonic acid (PTSA, 98.5+%), glutatic anhydride (95%), *n*-hexadecane (HD, 99%), and ethyl vinyl ether (99%) were purchased from Acros. L-Lactide (LA, 98%) and the second generation Grubbs catalyst were purchased from Aldrich. Tetrahydrofuran (THF; HPLC), diethyl ether (HPLC), methanol (HPLC), toluene (HPLC), dichloromethane (DCM; HPLC), ethyl acetate (EtOAc, HPLC), and triethylamine (99+%) were purchased from Fisher Chemical. α-Methyloxy ω-hydroxyl $PEO_{45}$ (PDI = 1.02) was purchased from RAPP Polymere. Toluene, DCM, and EtOAc were dried by distillation over $CaH_2$. LA was recrystallized from dry EtOAc four times prior to use. 4-(Dimethyleamino)pyridinium 4-toluenesulfonate (DPTS) was prepared by the reaction of equimolar amounts of DMAP and PTSA in THF. The third generation Grubbs catalyst and *exo*-NB-based diol **2** were synthesized according to the literature procedures.[36,45] All other chemicals were used without further purification unless stated otherwise.

**Synthesis of ω-Acid-Functionalized $PEO_{45}$, 1.** α-Methyloxy ω-hydroxyl PEO (4.00 g, 2.00 mmol) and glutaric anhydride (0.918 g, 8.00 mmol) were dissolved into 50 mL of DCM at 0 °C. A solution of triethylamine (0.607 g, 6.00 mmol) in 10 mL of DCM was added into the solution. The reaction was allowed for 5 h at 0 °C. Then the temperature was raised to room temperature, and the reaction was allowed for 19 h to reach full conversion. The reaction mixture was concentrated and precipitated in ether−methanol (99:1; v/v) three times to give **1** as a white solid. Yield: 95%. $^1$H NMR (500 MHz, $CDCl_3$, ppm): δ 1.95 (m, 2H, $CH_2CH_2CH_2$), 2.36−2.44 (m, 4H, $CH_2CH_2CH_2$), 3.38 (s, 3H, $CH_3O$), 3.47−3.70 (m, 178H, $OCH_2CH_2$ from PEO, except a $CH_2$ at the ω-terminal), 4.24 (t, 2H, $J$ = 6.0 Hz, $CH_2CH_2OCO$ at ω-terminal of PEO).

**Synthesis of PEO-Based NB-Functionalized Alcohol, 3.** *exo*-NB-based diol **2** (2.04 g, 4.73 mmol), DCC (0.342 g, 1.66 mmol), and DPTS (0.139 g, 0.473 mmol) were dissolved in 50 mL of DCM at 0 °C. The solution of **1** (2.50 g, 1.18 mmol) in 75 mL of DCM was added dropwise into the solution in more than 3 h. The reaction was allowed at 0 °C for 5 h. Then the temperature was raised to room temperature, and the reaction was allowed for 12 h to reach full conversion. After filtration, 100 mL of water was added into the reaction mixture, and the product was extracted with DCM for three times. The organic phase was concentrated and precipitated in ether−methanol (99:1; v/v) three times to give **3** as a white solid. Yield: 86%. $M_n^{NMR}$ = 2.55 kDa, $M_n^{GPC}$ = 7.35 kDa, $PDI^{GPC}$ = 1.02, $M_n^{MALDI}$ = 2.39 kDa, $PDI^{MALDI}$ = 1.06. $^1$H NMR (500 MHz, $CDCl_3$, ppm): δ 1.20 (s, 3H, $CH_3$ from **2**), 1.33−1.40 (m, 2H, 2 × 0.5 × $CH_2$ from NB of **2**), 1.53 (m, 1H, 0.5 × $CH_2$ from NB of **2**), 1.90−1.98 (m, 3H, $CH_2$ from **1** and 0.5 × $CH_2$ from NB of **2**), 2.24 (m, 1H, CH from NB of **2**), 2.37−2.42 (m, 4H, 2 × $CH_2$ from **1**), 2.92 (m, 2H, CH from NB of **2** and OH from **2**), 3.04 (m, 1H, CH from NB of **2**), 3.38 (s, 3H, $CH_3$ from **1**), 3.44−3.86 (m, 194H, all $OCH_2CH_2$, except $CH_2OCO$), 4.20−4.38 (m, 8H, 4 × $CH_2OCO$), 6.09−6.17 (m, 2H, CH=CH of NB from **2**).

**Synthesis of PEO-NB-PLA Diblock MMs 4.** The synthesis of **4b** is described as follows, and the other samples of MMs were prepared following the similar procedure. In a 10 mL Schlenk flask, **3** (2.41 g, 0.952 mmol), LA (3.43 g, 23.8 mmol), and DMAP (0.465 g, 3.81 mmol) were added under a nitrogen atmosphere. After dissolving the chemicals with 9.7 mL of DCM, the reaction was allowed for 15 h at 35 °C. By $^1$H NMR analysis of an aliquot of polymerization solution, 78% conversion of LA was estimated based on the resonance intensities of the CH protons of remaining LA monomer at 5.06 ppm relative to the CH protons of the resulting polymer at 5.18−5.32 ppm. Then the polymer solution was precipitated in ether−methanol (99:1; v/v) three times to give $PEO_{45}$-NB-$PLA_{22}$ **4b**. Isolation yield: 77% (based on 78% conversion of LA). $DP_{PLA}^{calcd}$ = 20, $DP_{PLA}^{NMR}$ = 22, $M_n^{calcd}$ = 5.32 kDa, $M_n^{NMR}$ = 5.70 kDa, $M_n^{GPC}$ = 17.1 kDa, $PDI^{GPC}$ = 1.05, $M_n^{MALDI}$ = 5.57 kDa, $PDI^{MALDI}$ = 1.05. $^1$H NMR (500 MHz, $CDCl_3$, ppm): δ 1.22 (s, 3H, $CH_3$ from **2**), 1.32−1.40 (m, 2H, 2 × 0.5 × $CH_2$ from NB of **2**), 1.43−1.79 (m, 133 H, all $CH_3$ of LA unit and 0.5 × $CH_2$ from NB of **2**), 1.89−1.99 (m, 3H, $CH_2$ from **1** and 0.5 × $CH_2$ from NB of **2**), 2.23 (m, 1H, CH from NB of **2**), 2.35−2.42 (m, 4H, 2 × $CH_2$ from **1**), 2.93 (m, 2H, CH from NB of **2** and OH from **2**), 3.05 (m, 1H, CH from NB of **2**), 3.38 (s, 3H, $CH_3$ from **1**), 3.45−3.86 (m, 192H, all $OCH_2CH_2$, except $CH_2OCO$), 4.12−4.41 (m, 11H, 5 × $CH_2OCO$ and CHOH of ω-terminal of PLA), 5.07−5.34 (m, 43H, all CH of LA except the one at ω-terminal of PLA), 6.08−6.17 (m, 2H, CH=CH of NB from **2**).

**Synthesis of PNB-*g*-PEO/PLA DBCs 5.** The synthesis of **5b1** is described as follows, and the other samples of DBCs were prepared following the similar procedure. In a 10 mL Schlenk flask, PEO-NB-$PLA_{22}$ **4b** (200 mg, 3.51 × $10^{-5}$ mol) was dissolved with 1.38 mL of DCM under a nitrogen atmosphere. After the addition of a DCM solution of the third generation Grubbs catalyst (1.0 mg/mL, 620 μL; 7.0 × $10^{-7}$ mol), the polymerization was allowed to react for 1 h at room temperature. Polymerization was quenched by the addition of a small amount of ethyl vinyl ether. Conversion of **4b** was determined as 96% by GPC analysis of an aliquot of the reaction mixture. The polymerization solution was precipitated in ether and redissolved by DCM, and then the resulting solution was eluted through silica gel (~2 g; pore size ~60 Å) using DCM as eluent. The first portion of eluted solution (~8 mL) was concentrated under reduced pressure to yield **5b1** as a white solid. Isolation yield: 68% (based on 96% conversion of **4b**). $DP_{PNB}^{calcd}$ = 48, $DP_{PNB}^{GPC}$ = 60, $M_n^{calcd}$ = 274 kDa, $M_n^{GPC}$ = 342 kDa, $PDI^{GPC}$ = 1.12. $^1$H NMR (500 MHz, $CDCl_3$, ppm): δ 1.18−1.75 (m, all $CH_3$ of LA unit, 2 × $CH_2$ and CH from PNB), 1.90−1.98 (m, $CH_2$ from **1**), 2.35−2.80 (m, 2 × $CH_2$ from **1** and 2 × CH from PNB), 3.39 (s, $CH_3$ from **1**), 3.49−3.81 (m, all $OCH_2CH_2$, except $CH_2OCO$), 4.10−4.42 (m, 11H, 5 × $CH_2OCO$ and CHOH of ω-terminal of PLA), 5.00−5.38 (m, all CH of LA except the one at ω-terminal of PLA, and CH=CH of PNB backbone).


dx.doi.org/10.1021/ma300565j | Macromolecules 2012, 45, 4623−4629

**Miniemulsion Surfactant Study.** Surfactant (DBCs **5b1**−**3** or MM **4b**), toluene, HD, and water were added to a vial ($W_{toluene}$:$W_{HD}$:$W_{DBC/MM}$ = 20:2:1; $V_{water}$:$V_{toluene/HD}$ = 225:1). After setting the vial in a water bath at room temperature, 20 min of ultrasonication was conducted for the mixture by using a 150 Series Digital Sonic Dismembrator (Fisher Scientific) equipped with a SLP Microtip (0.08 in. diameter, Brason Ultrasonics), operating at continuous mode with an amplitude of 60%. The sizes of the nanodroplets in the resulting miniemulsions were monitored by DLS. For each of the trials using **4b** and **5b2** as surfactants, 1.8 mL of the miniemulsion was transferred into a DLS cell at day 16. Then 1.2 mL of toluene was added slowly into the cell, and the nanodroplet sizes of the miniemulsion under the toluene layer were also monitored by DLS. The average cross-sectional interfacial area stabilized by surfactant ($A_{surf}$) was calculated as follows:

$$A_{surf}(\text{relative to } \mathbf{4b} \text{ molecule or unit}) = A_i/N_{\mathbf{4b}} = (6V_o/D)/(mN_A/M_{n,\mathbf{4b}})$$

in which $A_i$ is the interfacial area per unit volume of miniemulsion, $N_{4b}$ is the number of **4b** molecule or unit per unit volume of miniemulsion, $V_o$ is the volume of oil phase per unit volume of miniemulsion, $D$ is the diameter of oil droplets in miniemulsion, $m$ is the mass of surfactant per unit volume of miniemulsion, and $N_A$ is Avogadro's number.

## ■ ASSOCIATED CONTENT

### Ⓢ Supporting Information

GPC curves of DBC **5c2** before and after purification, GPC curves of sequential MM addition experiment, GPC curves of **4b** before and after using as miniemulsion surfactant, thermolytic profiles of **4b** and **5b2**. This material is available free of charge via the Internet at http://pubs.acs.org.

## ■ AUTHOR INFORMATION


### Corresponding Author

*E-mail: ccheng8@buffalo.edu.


### Notes

The authors declare no competing financial interest.

## ■ ACKNOWLEDGMENTS

The authors thank Prof. Javid Rzayev and Dr. Yueling Qin for kind assistance on characterization.

## ■ REFERENCES


(1) *Amphiphilic Block Copolymers: Self-Assembly and Applications*; Alexandridis, P., Lindman, B., Eds.; Elsevier: Amsterdam, Netherlands, 2000.

(2) de Gennes, P. G. *Rev. Mod. Phys.* **1992**, *64*, 645−648.

(3) Hawker, C. J.; Wooley, K. L.; Fréchet, J. M. J. *J. Chem. Soc., Perkin Trans. 1* **1993**, 1287−1297.

(4) Bo, Z.; Rabe, J. P.; Schlüter, A. D. *Angew. Chem., Int. Ed.* **1999**, *38*, 2370−2372.

(5) Walther, A.; Hoffmann, M.; Müller, A. H. E. *Angew. Chem., Int. Ed.* **2008**, *47*, 711−714.

(6) Walther, A.; Matussek, K.; Müller, A. H. E. *ACS Nano* **2008**, *2*, 1167−1178.

(7) Heroguez, V.; Gnanou, Y.; Fontanille, M. *Macromolecules* **1997**, *30*, 4791−4798.

(8) Zhang, M.; Müller, A. H. E. *J. Polym. Sci., Part A: Polym. Chem.* **2005**, *43*, 3461−3481.

(9) Sheiko, S. S.; Sumerlin, B. S.; Matyjaszewski, K. *Prog. Polym. Sci.* **2008**, *33*, 759−785.

(10) Chen, Y. *Macromolecules* **2012**, *45*, 2619−2631.

(11) Lanson, D.; Schappacher, M.; Borsali, R.; Deffieux, A. *Macromolecules* **2007**, *40*, 9503−9509.

(12) Li, Z.; Ma, J.; Cheng, C.; Zhang, K.; Wooley, K. L. *Macromolecules* **2010**, *43*, 1182−1184.

(13) Bolton, J.; Bailey, T. S.; Rzayev, J. *Nano Lett.* **2011**, *11*, 998−1001.

(14) Xia, Y.; Olsen, B. D.; Kornfield, J. A.; Grubbs, R. H. *J. Am. Chem. Soc.* **2009**, *131*, 18525−18532.

(15) Stephan, T.; Muth, S.; Schmidt, M. *Macromolecules* **2002**, *35*, 9857−9860.

(16) Neugebauer, D.; Zhang, Y.; Pakula, T.; Matyjaszewski, K. *Macromolecules* **2005**, *38*, 8687−8693.

(17) Zhang, Y.; Li, X.; Deng, G.; Chen, Y. *Macromol. Chem. Phys.* **2006**, *207*, 1394−1403.

(18) Wu, D.; Yang, Y.; Cheng, X.; Liu, L.; Tian, J.; Zhao, H. *Macromolecules* **2006**, *39*, 7513−7519.

(19) Zhu, H.; Deng, G.; Chen, Y. *Polymer* **2008**, *49*, 405−411.

(20) Xie, M.; Dang, J.; Han, H.; Wang, W.; Liu, J.; He, X.; Zhang, Y. *Macromolecules* **2008**, *41*, 9004−9010.

(21) Ishizu, K.; Sawada, N.; Satoh, J.; Sogabe, A. *J. Mater. Sci. Lett.* **2003**, *22*, 1219−1222.

(22) Yin, J.; Ge, Z.; Liu, H.; Liu, S. *J. Polym. Sci., Part A: Polym. Chem.* **2009**, *47*, 2608−2619.

(23) Lian, X.; Wu, D.; Song, X.; Zhao, H. *Macromolecules* **2010**, *43*, 7434−7445.

(24) Theodorakis, P. E.; Paul, W.; Binder, K. *Macromolecules* **2010**, *43*, 5137−5148.

(25) Xia, N.; Zhang, G.; Li, T.; Wang, W.; Zhu, H.; Chen, Y.; Deng, G. *Polymer* **2011**, *52*, 4581−4589.

(26) Li, Y.; Themistou, E.; Zou, J.; Das, B. P.; Tsianou, M.; Cheng, C. *ACS Macro Lett.* **2012**, *1*, 52−56.

(27) Sheiko, S. S.; Sun, F. C.; Randall, A.; Shirvanyants, D.; Rubinstein, M.; Lee, H.-i.; Matyjaszewski, K. *Nature* **2006**, *440*, 191−194.

(28) Cheng, C.; Yang, N.-L. *Macromolecules* **2010**, *43*, 3153−3155.

(29) Li, Y.; Themistou, E.; Das, B. P.; Christian-Tabak, L.; Zou, J.; Tsianou, M.; Cheng, C. *Chem. Commun.* **2011**, *47*, 11697−11699.

(30) Zou, J.; Hew, C. C.; Themistou, E.; Li, Y.; Chen, C.-K.; Alexandridis, P.; Cheng, C. *Adv. Mater.* **2011**, *23*, 4274−4277.

(31) Zou, J.; Yu, Y.; Yu, L.; Li, Y.; Chen, C.-K.; Cheng, C. *J. Polym. Sci., Part A: Polym. Chem.* **2012**, *50*, 142−148.

(32) Hadjichristidis, N.; Pitsikalis, M.; Iatrou, H.; Pispas, S. *Macromol. Rapid Commun.* **2003**, *24*, 979−1013.

(33) Johnson, J. A.; Lu, Y.-Y.; Burts, A. O.; Lim, Y.-H.; Finn, M. G.; Koberstein, J. T.; Turro, N. J.; Tirrell, D. A.; Grubbs, R. H. *J. Am. Chem. Soc.* **2011**, *133*, 559−566.

(34) Li, Z.; Ma, J.; Lee, N. S.; Wooley, K. L. *J. Am. Chem. Soc.* **2011**, *133*, 1228−1231.

(35) Zou, J.; Jafr, G.; Themistou, E.; Yap, Y.; Wintrob, Z. A. P.; Alexandridis, P.; Ceacareanu, A. C.; Cheng, C. *Chem. Commun.* **2011**, *47*, 4493−4495.

(36) Jha, S.; Dutta, S.; Bowden, N. B. *Macromolecules* **2004**, *37*, 4365−4374.

(37) Sun, G.; Fang, H.; Cheng, C.; Lu, P.; Zhang, K.; Walker, A. V.; Taylor, J.-S. A.; Wooley, K. L. *ACS Nano* **2009**, *3*, 673−681.

(38) Nederberg, F.; Connor, E. F.; Moeller, M.; Glauser, T.; Hedrick, J. L. *Angew. Chem., Int. Ed.* **2001**, *40*, 2712−2715.

(39) Cheng, C.; Khoshdel, E.; Wooley, K. L. *Nano Lett.* **2006**, *6*, 1741−1746.

(40) *Polymer Handbook*; Brandrup, J., Immergut, E. H., Grulke, E. A., Eds.; Wiley: New York, 1999.

(41) Landfester, K. *Macromol. Rapid Commun.* **2001**, *22*, 896−936.

(42) Landfester, K.; Musyanovych, A.; Mailänder, V. *J. Polym. Sci., Part A: Polym. Chem.* **2010**, *48*, 493−515.

(43) Scott, C.; Wu, D.; Ho, C.-C.; Co, C. C. *J. Am. Chem. Soc.* **2005**, *127*, 4160−4161.

(44) Akpo, C.; Weber, E.; Reicheb, J. *New J. Chem.* **2006**, *30*, 1820−1833.

(45) Love, J. A.; Morgan, J. P.; Trnka, T. M.; Grubbs, R. H. *Angew. Chem., Int. Ed.* **2002**, *41*, 4035−4037.